

## BIRD STRIKE DAMAGE ASSESSMENT FOR AN AIRCRAFT TAIL PLANE

Cătălin PÎRVU, Corina Elena BOȘCOIANU, Mihai Victor PRICOP, Lorena DELEANU

INCAS, Iuliu Maniu 220, 06126, Bucharest  
“Dunarea de Jos” University of Galati

Pirvu.catalin@incas.ro

### Abstract

*Bird strike is a major threat to both fixed and rotary wing aircraft, damaging the nose section, wings, or propulsion elements. It involves a complex material failure under dynamic loads. The purpose of this work is to perform numerical predictions in the case of a horizontal tail plane, considering a number of span wise impact locations. Three types of water birds are considered, using a Lagrangian model, shaped as a rounded cylinder. A bilinear isotropic material with failure criterion is considered, in order to overcome the numerical problems typically related to the large displacements of Lagrangian models. Simulations help to locate the most damaged zones and are helpful for improving the structure design by changing the position and size of the structural members. The results are going to be correlated with accident records in order to better understand safety requirements.*

**Keywords:** bird strike, aircraft, failure, FEM model, bilinear isotropic material, equivalent plastic strain

### 1. INTRODUCTION

Costs associated with bird-aircraft collisions affect commerce and safety and are widely acknowledged by the aviation community [1, 2, 3, 4, 5]. Several well documented reports as that of Nikolajeff [6], Kirsh et al. [7], Doubrava and Strnad [32] pointed out that the bird collision is a high risk issue for airplanes (Fig. 1) and solutions are needed, including mitigating the structure failure under the impact. The annual direct costs (aircraft repair costs) associated with bird strikes in the US have been estimated at US\$ 155 million [2]. These authors considered that is likely a substantial underestimate of the magnitude of the problem. FAA Wildlife Database 1990-2014 evaluate that there were 917 strikes produced by gulls (\$65 K), 659 Canadian goose strikes (\$381 K), 292 strikes by Turkey vulture (\$74 K) [3].

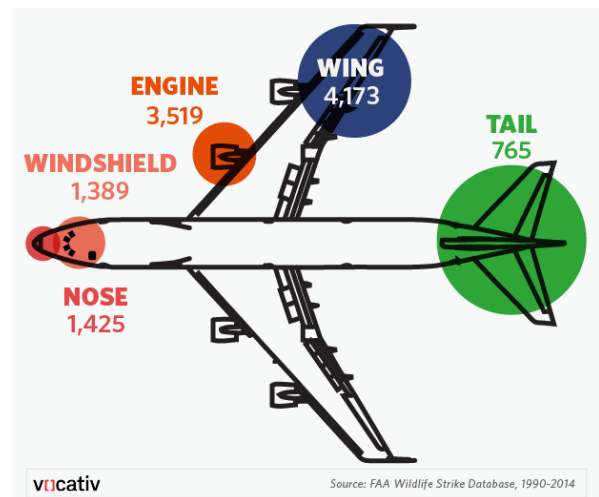


Fig. 1. Parts of the plane wildlife hit most often [3]

Anderson et al. [8] provides a model for better understanding of how the probability and extent of damage are affected by the characteristics of a bird strike. The model can be used to estimate the cost of

the substantial number of strikes for which the actual cost is unreported. Thus, the goal of future work will be to better assess how the cost of bird strikes varies across airports and over time by using this model to alleviate the problem of underreporting of strike costs present in current data.

Ugrcic [9] did a numerical simulation using smooth particle hydrodynamics (SPH) method running in the nonlinear finite element code ANSYS AUTODYN. The focus is given to the validation of the stress, strain and deflection of wing on the impact zone. The dependency of parameters on the variation of ellipsoidal bird aspect ratio, impact velocity and wing design details were discussed. The behavior of aircraft leading edge against high speed bird impact was simulated and the effect of parameters on its dynamic response was studied. Numerical model was validated with published experimental results.

Sun [10] performed numerical predictions of structural behavior and damage caused by bird strikes in a large airplane leading edge structure, at different locations, using smooth particle hydrodynamics (SPH) method. A dynamic failure model with effects of complex stress states and strain rate was implemented and appropriate contact definitions between the bird and structure were used. The results showed that the failure of leading edge structure under bird strike can be effectively simulated for an impact velocity of 80...170 m/s. Simulations of bird strike on an aircraft leading edge structure at three different locations along with the span of wing were performed. and showed that the impact damage was dependent on the impact location. In order to deal with the numerical prediction, behavior and damage caused by bird strikes in a horizontal empennage structure using finite element method, interactions of several complex numerical problems are involved.

Different bird modeling techniques appeared in recent years having apparent effects on the results of simulations and experimental validation [11, 12, 13, 14], which is essential to predict the damage caused by bird impact.

The three commonly used approaches to simulate the bird impact case are: the Lagrangian approach, the Arbitrary Lagrangian Eulerian (ALE) approach and the Smooth Particle Hydrodynamics (SPH) method [15].

In Lagrange approach, the mesh moves and distorts once with the material. This formulation is often used because of the advantages of being able to incorporate complex material models and the ability to accurately model interfaces for the empennage and changing in the bird's body. The

method is generally used for shaping solid materials, but is very sensitive to deformation, can produce small time steps (at interaction bird-empennage) and even numerical divergence.

Computing codes solve these problems by remeshing algorithms or erosion of highly distorted elements, using typically a threshold (this can have different nature, usually a stress or deformation). Remeshing algorithms requiring a large amount of calculation are not applicable in all cases. On the other hand, erosion algorithms can cause loss of accuracy by removing highly distorted elements. The amount of mass that disappears it also affects the inertial properties of the model. Problems may arise due to erosion and contact interfaces.

Zhang et al. [16] found that bird geometry and impact orientation had significant effects on impact response and kinetic energy loss of the bird. Simulation of a bird impact on a rotary jet-engine fan were done taking into account impact force history, kinetic energy loss of the bird, deformations of the blade tips and von Mises stresses of the blade roots. The results showed that both bird geometry and impact orientation had significant influence.

Remeshing techniques are generally used to simulate the impact, penetration, blast, fragmentation, and problems of turbulent fluid-structure interaction that occurs, making this technique a reliable method for our case of bird-empennage impact.

## 2. THE MODEL

In order to ensure tolerance to bird strike damage, aircraft structures have to fulfill the airworthiness specifications prescribed by Federal Aviation Administration, Joint Aviation Authorities or the European Organisation for the Safety of Air Navigation, imputing tests on new and old structures that can be made with air canon and numerical simulation.

The case chosen is an IAR-330 helicopter catastrophic flight event. The impact case between different bird bodies and horizontal empennage lead to the unnatural rupture of the empennage, indicating a rupture direction at the base of the empennage and a destroyed structure for front impact. The empennage damage at a lower height, during flight, could have caused the loss of vertical stability of the helicopter.

The empennage is fixed (clamped) on the top left helicopter tail on the opposite side of the tail rotor (Fig. 1a).

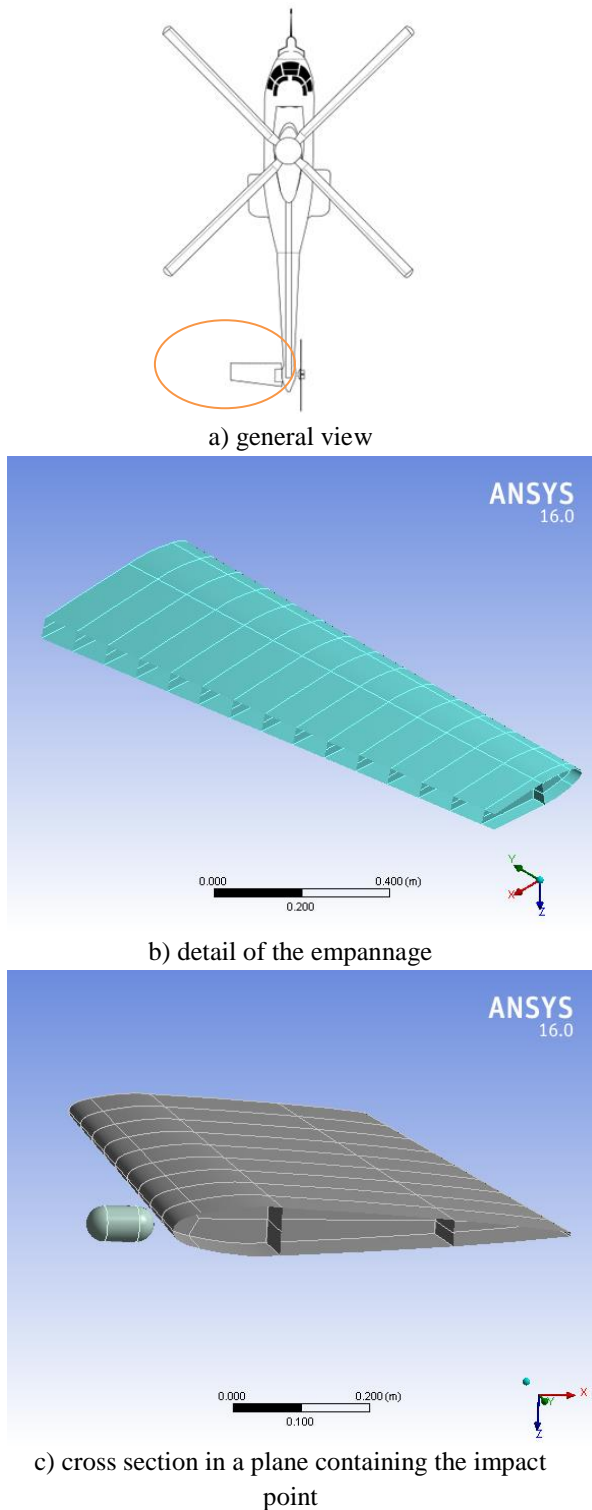


Fig. 2. IAR 330 horizontal empennage with 2 section planes

For accurate results, considering the aeronautical domain, which covers specific issues of the thin-walled structures used in aviation, the modeling of the empennage only with "shell" type finite elements

was chosen. The constitutive material of the empennage is Al-2024 aluminum alloy, commonly used in the aircraft industry. The structure thickness is 1 mm in this model, and it is composed of 20721 nodes and 19907 elements. The bird model (a cylinder with spherical ends) has 4770 nodes and 23855 elements. The properties of these two materials involved in the simulations are given in Table 1. Bird properties were selected after consulting relevant documentation [A11].

An actual bird has an irregular shape and also the body density varies. For laboratory test, there are used artificial birds or substitute birds for pre-certification impact testing, leading to advantages in convenience, cost and reproducibility [19].

The substitute bird shall not copy the real bird itself with its flesh and bones, but it should reproduce the same pressure loading during impact as a real bird. The substitute bird geometry and material have to be selected appropriately for this purpose.

Typical substitute artificial birds have a simplified regular geometry like a cylinder, a cylinder with hemispherical ends [20], an ellipsoid or a sphere, representing the torso of the bird. For this study, the authors selected the cylinder with hemispherical ends.

Several authors tried to model the bird with a simple elastoplastic material law with a defined failure strain [21, 22, 23], and some of them highlighted the limitations of this simplified approach. It is observed that no fluid-like flow response can be achieved with such an elasto-plastic material law, only if the shear modulus  $G$  is set very low. The determination of the material constants is reported to be difficult and of key importance. However, no comparison to results obtained with traditional bird models is given [24].

In order to describe the mechanical behavior of this empennage material and an organic body in dynamic conditions, the bilinear isotropic material model was selected, with a failure criterion defined by the maximum equivalent plastic strain, EPS.

Table 1. Material properties

Property	Bird	Al 2024
Density, $\text{Kg}\cdot\text{m}^{-3}$	950	2785
Young Modulus, MPa	10000	71000
Poisson Ratio	0.3	0.33
Bulk Modulus, MPa	8333	6.9608
Shear Modulus, MPa	3846	26692
Yield strength, MPa	106	280
Tangent Modulus, MPa	5 000	500
Maximum equivalent plastic strain, EPS	1.25	0.7

### The mesh network

The assembly was discretized using the Lagrangian method, with a maximum element size of 10 mm. Following the meshing process, the statistics for the empennage are 47358 nodes and 48802 elements, and the birds, with a defined number of elements and nodes (Table 2).

### The initial conditions

The relative speed of the bird before impact was set at 100 m/s, a value in the actual range for these birds [11, 31]. Erosion is used to automatically remove highly distorted elements from the analysis and is required for this kind of applications. The default settings will erode elements which experience geometric strains in excess of 100%. The friction coefficient is set to 0.3.

### Boundary conditions and analysis settings

The empennage has the root surfaces clamped. The simulation time was different, depending on the bird model size,  $4.5 \times 10^{-3}$  s for 0.17 kg,  $55 \times 10^{-3}$  s for 1.2 kg and  $5 \times 10^{-3}$  for the largest one (12 kg) with a program control time step.

## 3. THE RESULTS

Numerical failure prediction of bird strike on a helicopter horizontal tail structure was simulated in Ansys Autodyn. The birds are modeled in line with the literature [25, 26, 27, 28, 29]. The largest bird taken into account in this simulation was modeled as a cylinder with spherical ends.

Table 2.

Bird	Mass	Speed	Nodes	Elements
Seagull	170 g	100 m/s	444	330
Duck	1.2 kg	100 m/s	4770	23855
Swan	12 kg	100 m/s	27448	145862

Analyzing the time history of equivalent stress in time (Fig. 3), one may notice that for the smaller bird models, a) and b), produced similar results: a sharp rise that last about  $1.5 \times 10^{-4}$  s for the seagull,  $2.5 \times 10^{-4}$  s for the duck, followed by a bump, with the peak still under the yield limit. The integration time is longer for the heavier bird with the oscillations being very probably produced by the stress propagation in the structure. The plot characterizing the heaviest bird has a different shape when compared to the smaller ones. After the sharp rise to similar value as for the other bird models, till around 500 MPa, there is a plateau till  $10^{-3}$  s and then after, in a short period of  $2.5 \dots 3 \times 10^{-4}$  s, the stress reaches the failure limit of the material (that is there are great deformations beyond the EPS imposed in the model and there are places in the structure that have ruptures.

The plots in Fig. 3 are similar to those given by Hu [Hu, 2016] near the impact point, even if those in Fig. 3 point out that high stress values could be also obtained farway from the impact zone (see zone B in Fig. 6c).

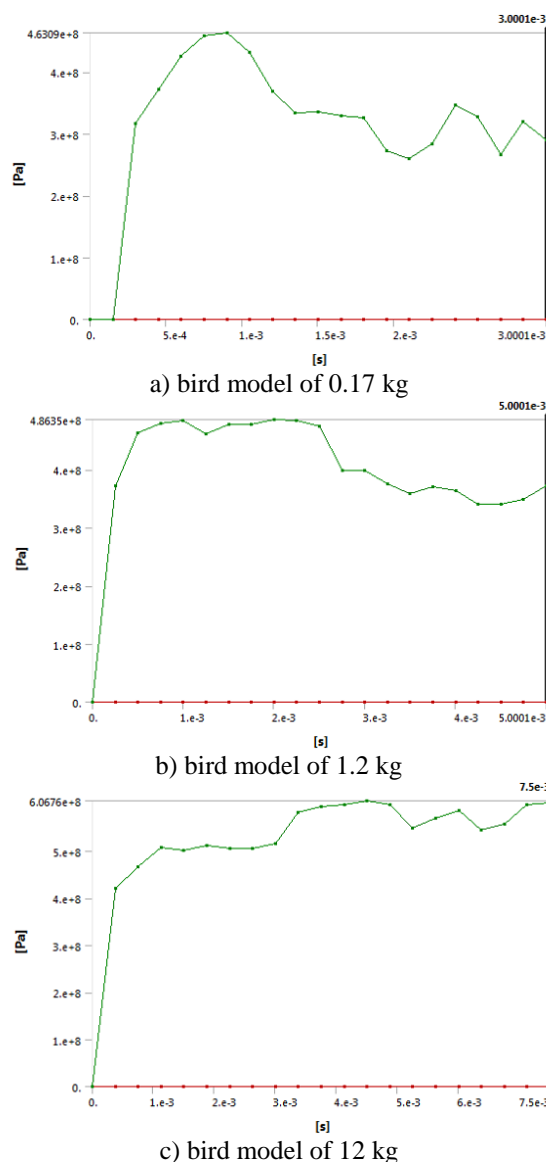
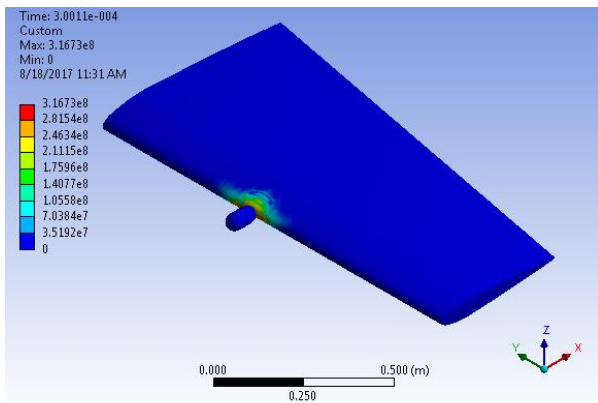


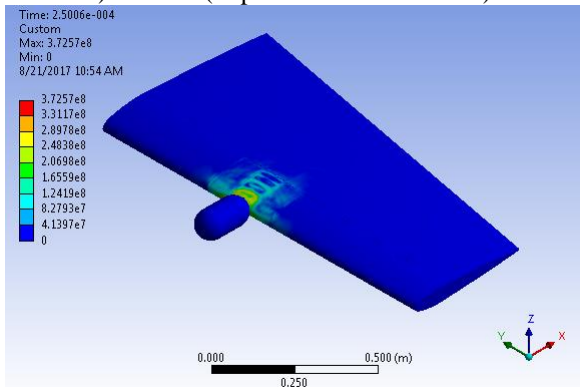
Fig. 3. Von Mises maximum stress during the impact

Material failures can be identified in the time histories of maximum von Mises stress. As stress is still near the failure limit, at the moment  $7.5 \times 10^{-3}$  s, it is very probably that rupture point are still developing and the integration time has to be enlarged for getting the last failure of the structure.

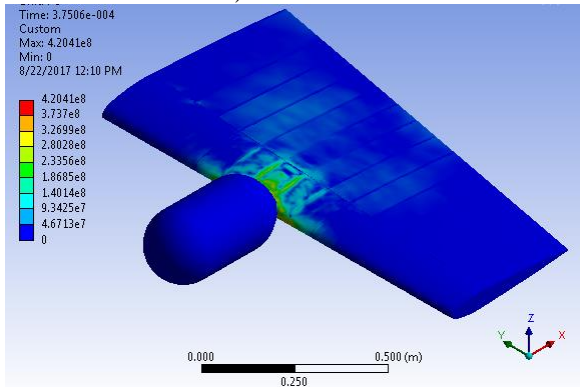
Figure 4 presents the moments at the end of first stage, for each case.



a)  $3 \times 10^{-4}$  s (impact starts at  $1.5 \times 10^{-4}$  s)



b)  $2.5 \times 10^{-4}$  s



c)  $3.75 \times 10^{-4}$  s

Fig. 4. Equivalent (von Mises) stress distribution (the moment at the end of first stage) [Pa]

As pointed out in literature, the impact behavior consists of four main phases: initial shock at contact, impact shock decay, steady flow and pressure decay [30, 31].

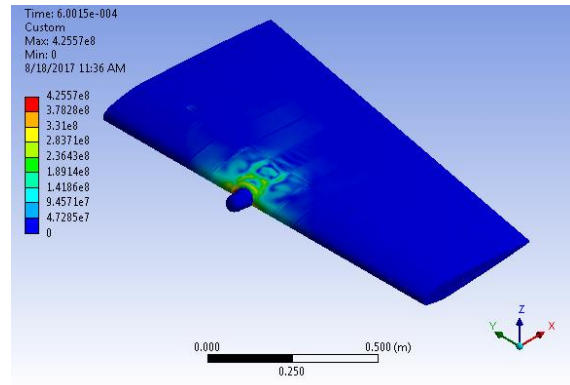
Thus, the impact process could be divided four stages:

- I a very sharp rise of the stress (initial shock at contact) (Fig. 4),
- II a stress slope smaller till 60...80% of the failure stress (Fig. 5),

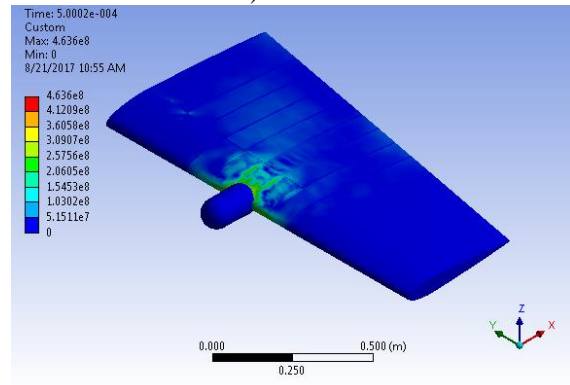
- III a hill shape of stress that is longer in time when the deformed bird mass increases;

- IV - decreasing stress (obviously in Fig. 3a and b, but not included in the integration time for the simulation with swan model).

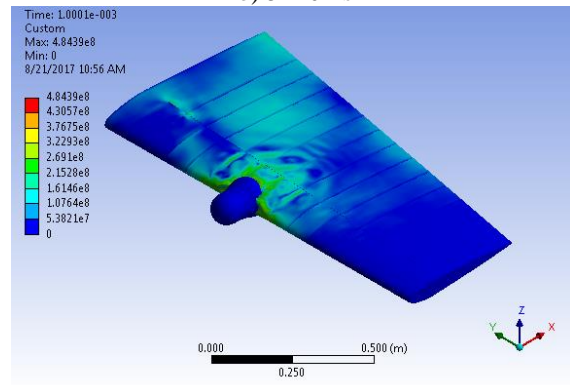
Figure 5 presents the end of the second stage that is the moment of reaching 60...80% of the failure stress limit, but the end of this stage is at different moments, for each simulated case.



a)  $6 \times 10^{-4}$  s



b)  $5 \times 10^{-4}$  s



c)  $10 \times 10^{-4}$  s

Fig. 5. The moment at the end of stage II (von Mises stress distribution) [Pa]

Figure 6 presents the instants when the maximum stress is reached in each case, without broking the structure.

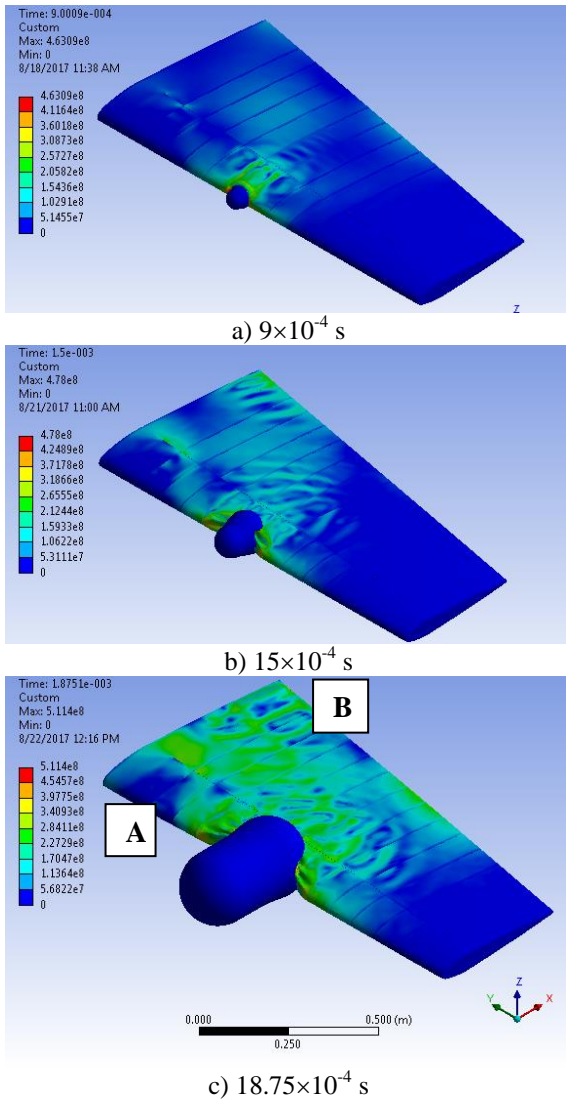


Fig. 6. The moment when the maximum stress is reached

The bending moment induced by the largest bird model makes the structure experience failure near the fixing plane (noted A in Fig. 6c). Here, tensile stresses are more dangerous and make the structure to fail and the surface of the structure in zone B is noticeably wrinkled. This process become more and more obviously and change in a very sever way the structure configuration.

The moment at which the von Mises stresses are the highest for the third case is given in Fig. 6. The reinforcing ribs inside the structure become stress concentrators (Fig. 8).

This simulation for the impact with a large bird suggests that symmetrical and uniform arrangement of structure elements is not beneficial for the structure resilience. Even if this arrangement is easy to manufacture, the design engineer could imagine a structure with a denser rib distribution near the empenage root.

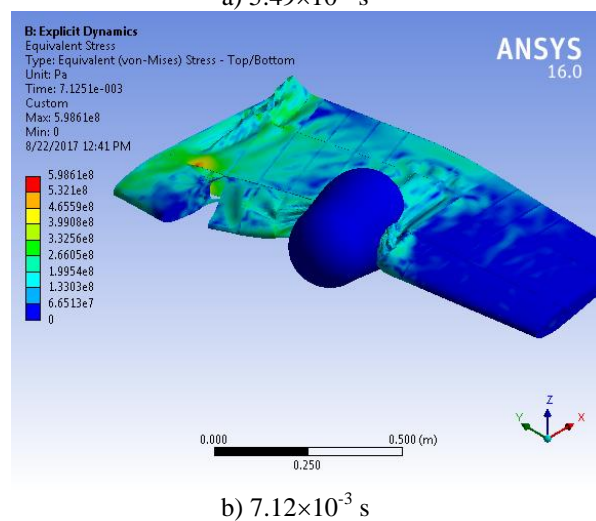
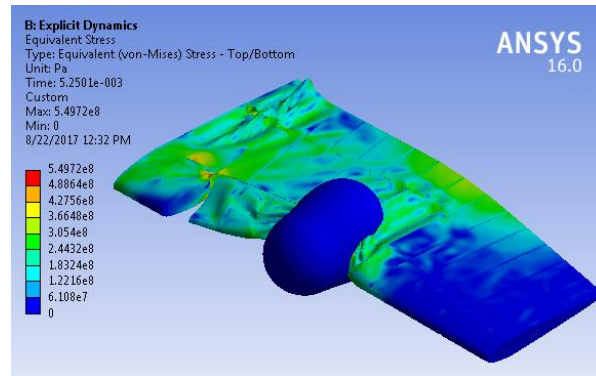
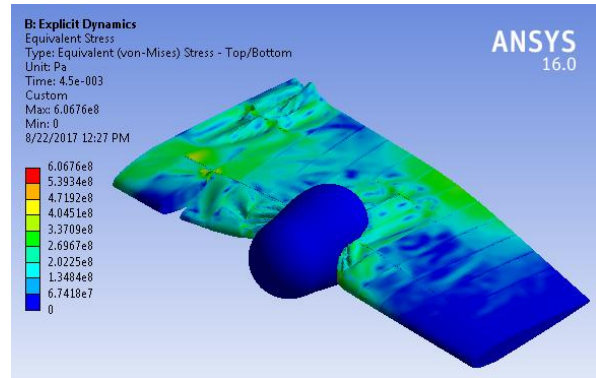


Fig. 8. Stress concentrations for two different moments, for the bigger bird model

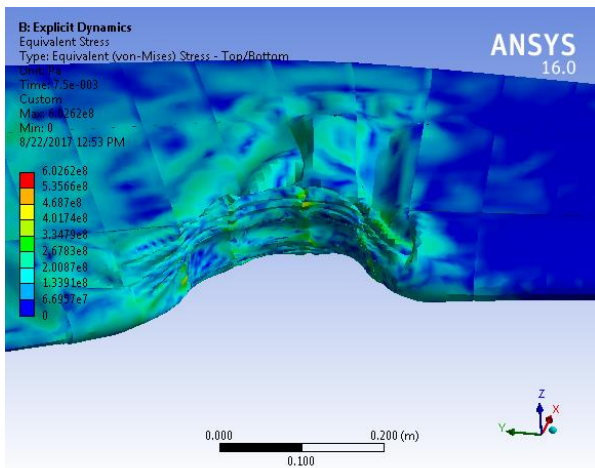
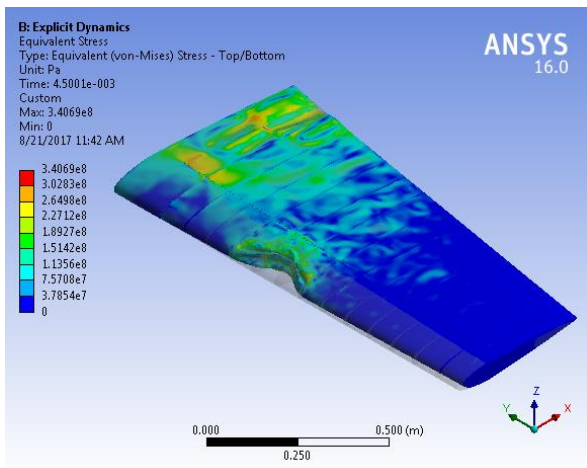
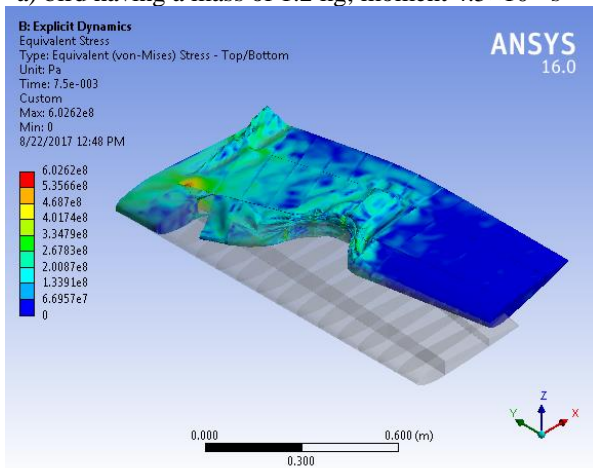


Fig. 9. Detail with bird as transparent body, at moment  $7.5 \times 10^{-3}$  s



a) bird having a mass of 1.2 kg, moment  $4.5 \times 10^{-3}$  s



b) bird having a mass of 12 kg, moment  $7.5 \times 10^{-3}$  s

Fig. 10. General views comparing the position of the structure before and after the impact

When analysing the stress distribution in the structure that bears the direct impact, one may notice that even if there are high values, the structure has high deformations but the integrity of the zone is kept (no broken material in this zone).

Figure 10 presents general views comparing the position of the structure before being struck and after the impact. The zone B is acutely folded at moment  $7.5 \times 10^{-3}$  s. There is no failure of the skins composing the structure, except the visible one (zone A), but the shape of the empannage is seriously changed. A smaller bird (1.2 kg) produces a position change of the structure of much lower variation. Figure 11 presents the folded zone behind the impact and near the fixing region.

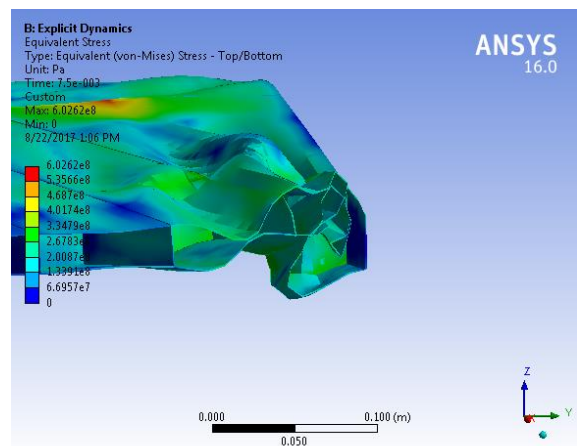


Fig. 11. Detail of acutely folded zone B at moment  $t = 7.5 \times 10^{-3}$  s.

One may compare Fig. 9 to the image in Fig. 13 [3] and could notice some similarities, but also differences in failure. The depth of the bird penetration in the structure is similar, but the actual structure is broken, not compressed (the structure is lighter than that analysed in the model). Also, the empannage is detached from the mounting surface and not broken as in the simulation. This aspect difference is due to boundary condition (the model used a stiff clamping boundary condition and ignores the aerodynamic loading).

Simulation helps engineer to analyze the failure process. For instance, during the impact, the maximum stress is not located in a single zone, but, in time, the maximum value appears to migrate. At moment  $t = 3 \times 10^{-4}$  s, the maximum value of von Mises stress appears just in the initial central contact, but then, this maximum value is laterally positioned at  $t = 10.5 \times 10^{-4}$  s and only after  $6 \times 10^{-4}$  s, this is found up and down in the impact zone. For small birrds, the simulation pointed out the rebound of the bird model.

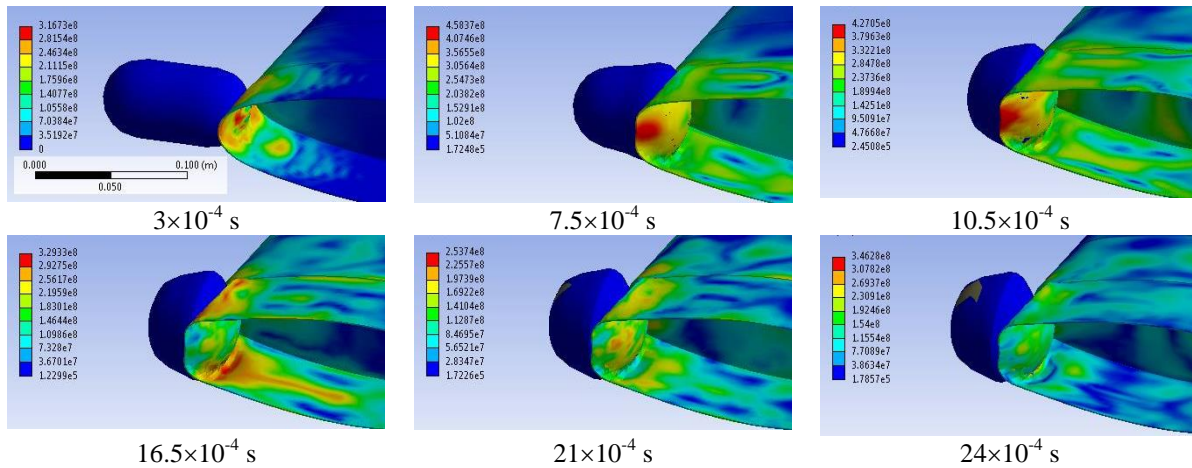


Fig. 12. von Mises stress distributions during the impact with the bird model of 0.17 kg [Pa]



Fig. 13. A bird strike in the upper surface of the wing structure [3]

The importance of simulation may be underlined by actual failure of similar structures, as for instance, for wing and tail, see Fig. 13. A bird strike in the upper surface of the wing structure generates a type of failure similar to simulation. The pilot returned the aircraft to airport and made an overweight landing. Cost of repairs was \$100,000. Bald eagles have a mean body mass of 4 kg for males and 5.5 kg for females [3].

Figure 14 presents a bird impact that folded the upper part of the wing. There are qualitative similarities between this photo and the folded zone in the models here presented.

#### 4. Conclusions

In these impact cases, bilinear hardening material models were implemented to simulate the failure of the structure.



Fig. 14. A CRJ 100/200 on departure from a Minnesota airport hit a soaring bald eagle at 5000 feet AGL on March 31<sup>st</sup> 2015, causing major damage to leading edge of wing [2]

This type of simulation uses erosion to remove distortion elements (generating numerical instabilities) and a criterion of failure based on maximum equivalent plastic strain (EPS).

In order to obtain reliable numerical results, the element size in the impact zone was refined with a size of 5 mm.

The results can be qualitatively validated with the image of the bird impact incidents.

The simulations help locate the most damaged zones and are helpful for improving the structure design by changing the positioning/sizing of the structural members. Simulations help to locate the most damaged zones and are helpful for improving the structure design by changing the positioning of the reinforcement elements. Also, simulation is helpful to investigate accidents, if the structure and some impact information is available.

These simulations help the designer to improve the impact resilience/robustness of the structure, pointing out critical sections, even if the initial conditions are simplified. For instance, here, the structure is considered as fixed in the tail and aerodynamic loads are neglected.

## REFERENCES

- Dolbeer R. A., 2013, The history of wildlife strikes and management at airports. pp. 1–6. in: DeVault T. L., Blackwell B.F., Belant J. L. (Eds.), *Wildlife in Airport Environments: Preventing Animal-Aircraft Collisions through Science-based Management*. John Hopkins University Press, Baltimore, MD, USA, p. 181.
- Dolbeer R. A., Weller J. R., Anderson A. L., Begier M. J., 2015, *Wildlife Strikes to Civil Aircraft in the United States, 1990–2015*, [https://www.faa.gov/airports/airport\\_safety/wildlife/media/Wildlife-Strike-Report-1990-2015.pdf](https://www.faa.gov/airports/airport_safety/wildlife/media/Wildlife-Strike-Report-1990-2015.pdf)
- \*\*\* Bird Strike, november 7, 2002 by gruntdoc, <http://gruntdoc.com/2002/11/bird-strike.html#sthash.ZTC236Fw.dpbs>
- Blackwell B. F., DeVault T.L., Fernández-Juricic E., Dolbeer R. A., 2009, Wildlife collisions with aircraft: a missing component of land-use planning on and near airports? *Landscape Urban Plan*, 93/1, pp. 1–9, <http://dx.doi.org/10.1016/j.landurbplan.2009.07.005>.
- Lopez-Zuazo M.L.-L. et al., 2016, A predictive model for risk assessment on imminent bird strikes on airport areas, *Aerosp. Sci. Technol.*, <http://dx.doi.org/10.1016/j.ast.2016.11.020>
- Nikolajeff J. P., 2014, Analysis of the Bird Strike Reports Received by the Finnish Transport Safety Agency between the Years 2000 and 2011, *Trafin tutkimuksia Trafis undersökningsrapporter, Trafi Research Reports 7/2014*
- Krisch J. A., Fox E. J., Reznik T., 2015, The Birds (And Deer) Behind Thousands Of Airplane Emergencies, A bird strike in the upper surface of the wing structure, <http://www.vocativ.com/culture/science/bird-strikes-airplane-faa-database/>
- Anderson A., Carpenter D. S., Begier M. J., Blackwell B. F., DeVault T. L., Shwiff S. A., 2015, Modeling the cost of bird strikes to US civil aircraft, *Transportation Research Part D* 38, pp. 49–58.
- Ugrčić M., Maksimović S. M., Stamenković D. P., Maksimović K. S., Nabil K., 2015, Finite Element Modeling of Wing Bird Strike, *FME Transactions* 43, pp. 82-87
- Sun Q., Liu Y. J., Jin R. H., 2014, Numerical simulation of bird strike in aircraft leading edge structure using a new dynamic failure model, 29th Congress of the International Council of the Aeronautical Sciences, St. Petersburg, Russia, September 7-12.
- Allaëys F., Luyck G., Van Paepegem W., Degrieck J., 2016, Characterization of real and substitute birds through experimental and numerical analysis of momentum, average impact force and residual energy in bird strike on three rigid targets: A flat plate, a wedge and a splitter, *Intern. J. of Impact Engineering* 99, 113
- Allaëys F., Luyck G., Van Paepegem W., Degrieck J., 2016, Development and validation of a set-up to measure the transferred multi-axial impact momentum of a bird strike on a booster vane, *International Journal of Impact Engineering* 99, pp. 102-110.
- Pahange H., Abolbashari M. H., 2016, Mass and performance optimization of an airplane wing leading edge structure against bird strike using Taguchi-based grey relational analysis, *Chinese Journal of Aeronautics*, 29/4, pp. 934–944
- Goyal V. K., Huertas C. A., Vasko T. J., 2013, Bird-Strike Modeling Based on the Lagrangian Formulation Using LS-DYNA, *American Transactions on Engineering & Applied Sciences*.
- Năstăsescu V., 2012, *Metoda SPH (Smoothed Particle Hydrodynamics)*, Editura Academiei Forțelor Terestre “Nicolae Bălcescu”, Sibiu.
- Zhang D., Fei Q., 2016, Effect of bird geometry and impact orientation in bird striking on a rotary jet-engine fan analysis using SPH method, *Aerospace Science and Technology* 54, pp. 320–329.
- \*\*\* <https://global.ihs.com/standards.cfm?publisher=JAA>
- \*\*\* The European Organisation for the Safety of Air Navigation
- Budgey R., 2000, The development of a substitute artificial bird by the International Birdstrike Research Group for use in aircraft component testing, *International Bird Strike Committee ISBC25/WP-IE3*, Amsterdam, The Netherlands.
- Dar U. A., W. Zhang, Xu Y., 2013, FE Analysis of Dynamic Response of Aircraft Windshield against Bird Impact, *Hindawi Publishing Corporation International Journal of Aerospace Engineering*, ID 171768, <http://dx.doi.org/10.1155/2013/171768>
- Zhu S, Tong M, Wang Y., 2009, Experiment and numerical simulation of a full-scale aircraft windshield subjected to bird impact. In: 50th AIAA/ASME/ASCE/AHS/ ASC Structures, structural dynamics, and materials conference, Palm Springs, CA, May 4–7.
- Hachenberg D, Graf O, Leopold T., 2003, Comparison of different approaches for bird strike simulation. In: 2nd EADS Workshop on crash and impact simulation, Ottobrunn, Germany, December 11.
- Zhang Y, Li Y., 2008, Analysis of the anti-bird impact performance of typical beamedge structure based on ANSYS/LS-DYNA. *Adv Mater Res* 33– 37, pp.395–400.
- Heimbs S., 2011, Computational methods for bird strike simulations: A review, *Computers and Structures* 89, pp. 2093–2112
- Hu D., Song B., Wang D., Chen Z., 2016, Experiment and numerical simulation of a full-scale helicopter composite cockpit structure subject to a bird strike, *Composite Structures* 149, pp. 385–397.
- Wang F. S., Yue Z. F., Yan W. Z., 2011, Factors study influencing on numerical simulation of aircraft windshield against bird strike, *Shock and Vibration* 18, pp. 407–424 4, DOI 10.3233/SAV-2010-0522 IOS Press.

27. Heimbs S., Bergmann T., 2012, High-Velocity Impact Behaviour of Prestressed Composite Plates under Bird Strike Loading, Hindawi Publishing Corporation International Journal of Aerospace Engineering, ID 372167, doi:10.1155/2012/372167
28. Huertas-Ortecho C. A., 2006, Robust Bird-Strike Modeling Using LS-DYNA, PhD thesis, University of Puerto Rico Mayagüez Campus.
29. Dede O., 2015, Investigation of Effects of Bird Strike on Wing Leading Edge by Using Explicit Finite Element Method, PhD, Middle East Technical University,  
file:///C:/Users/Lorena%20Deleanu/Documents/Downloads/383073.pdf
30. Martin N. F., 1990, Nonlinear finite-element analysis to predict fan-blade damage due to soft-body impact. J Propul Power 6/4, pp.445–50.
31. Anghileri M., Sala G., 1996, Theoretical assessment, numerical simulation and comparison with tests of birdstrike on deformable structures. In: Proceedings of the 20th ICAS congress, Sorrento, Italy, September 8–13, pp. 665–74.
32. Doubrava R., Strnad V., 2010, Bird strike analyses on the parts of aircraft structure. In: ICAS 2010, 27th Congress of the Intern. Council of the Aeronautical Sciences, Nice, France, September 19–24.